DALTON
FULL PAPER

Synthesis of four derivatives of 3,6,10-tri(carboxymethyl)-3,6,10-triazadodecanedioic acid, the stabilities of their complexes with Ca(II), Cu(II), Zn(II) and lanthanide(III) and water-exchange investigations of Gd(III) chelates †

Tsan-Hwang Cheng,[a] Yun-Ming Wang,*[a] Kuei-Tang Lin[a] and Gin-Chung Liu[b]

[a] *School of Chemistry, Kaohsiung Medical University, 100 Shih-Chuan 1st Road, Kaohsiung, Taiwan 807, Republic of China*
[b] *Department of Radiology, Kaohsiung Medical University, 100 Shih-Chuan 1st Road, Kaohsiung, Taiwan 807, Republic of China*

Received 2nd August 2001, Accepted 6th September 2001
First published as an Advance Article on the web 26th October 2001

The protonation constants of four poly(aminocarboxylates), *N*′-pyridylmethyl (TTDA-PY), *N*′-2-hydroxypropyl (TTDA-HP), *N*′-2-hydroxy-1-phenylethyl (TTDA-H1P) and *N*′-2-hydroxy-2-phenylethyl (TTDA-H2P) derivatives of TTDA (3,6,10-tri(carboxymethyl)-3,6,10-triazadodecanedioic acid), and the stability constants of their complexes formed with Ca^{2+}, Zn^{2+}, Cu^{2+}, La^{3+}, Ce^{3+}, Nd^{3+}, Sm^{3+}, Gd^{3+}, Dy^{3+}, Ho^{3+}, Yb^{3+} and Lu^{3+} were determined by potentiometric methods at 25.0 ± 0.1 °C and 0.10 mol dm^{-3} ionic strength in Me_4NNO_3. The stability of the Gd(III) complexes follows the order TTDA-PY > TTDA-H2P ≈ TTDA-HP ≈ TTDA-H1P. The thermodynamic resistance of the gadolinium(III) complexes, at the plasma concentration used in clinical applications, towards demetallation in the presence of important components of blood plasma, such as Ca(II), Zn(II) and Cu(II), has been evaluated. The observed water proton relaxivity values of $[Gd(TTDA\text{-}PY)]^-$, $[Gd(TTDA\text{-}HP)]^-$, $[Gd(TTDA\text{-}H1P)]^-$ and $[Gd(TTDA\text{-}H2P)]^-$ became constant with respect to pH changes over the range of 4–10, 6–10, 6–10 and 6–10, respectively. ^{17}O NMR shifts showed that the $[Dy(TTDA\text{-}PY)]^-$, $[Dy(TTDA\text{-}HP)]^-$, $[Dy(TTDA\text{-}H1P)]^-$ and $[Dy(TTDA\text{-}H2P)]^-$ complexes at pH 6.30 and 4.30 had 0.9 and 0.9; 2.2 and 3.4; 2.0 and 3.5; 1.8 and 3.0 inner-sphere water molecules, respectively. Water proton spin–lattice relaxation rates for gadolinium(III) complexes were also consistent with the number of inner-sphere water molecules. The EPR transverse electronic relaxation rate and ^{17}O NMR transverse relaxation time were thoroughly investigated and the results obtained were compared with that previously reported for the other gadolinium(III) complex, $[Gd(DTPA)(H_2O)]^{2-}$. Short exchange lifetime values were obtained for the $[Gd(TTDA)(H_2O)]^{2-}$, $[Gd(TTDA\text{-}PY)(H_2O)]^-$, $[Gd(TTDA\text{-}HP)(H_2O)_2]^-$, $[Gd(TTDA\text{-}H1P)(H_2O)_2]^-$ and $[Gd(TTDA\text{-}H2P)(H_2O)_2]^-$ complexes. Their water-exchange rates are about 24–45 times faster than that for the $[Gd(DTPA)(H_2O)]^{2-}$ complex, which suggested that the longer backbone of the multidentate ligand may be pulled tightly into the first coordination sphere, resulting in high steric constraints at the water binding site.

Introduction

The use of paramagnetic metal complexes as contrast agents for magnetic resonance imaging (MRI) have been developed very rapidly and extensively.[1–3] The octachelating ligands, 3,6,9-tri(carboxymethyl)-3,6,9-triazadodecanedioic acid (DTPA), 1,7-bis[(*N*-methylcarbamoyl)methyl]-1,4,7-triazaheptane-1,4,7-triacetate (DTPA-BMA), 10-(2-hydroxypropyl)-1,4,7,10-tetraazacyclododecane-1,4,7-triacetic acid (HP-DO3A), 1,4,7,10-tetraazacyclododecane-*N*,*N*′,*N*″,*N*‴-tetraacetic acid (DOTA), 3,6,9-triaza-3,6,9-tris(carboxymethyl)-4-(4-ethoxybenzyl)undecandicarboxylic acid (EOB-DTPA), 1,4,7-tris(carboxymethyl)-10-(1-(hydroxymethyl)-2,3-dihydroxypropyl)-1,4,7,10-tetraazacyclododecane (DO3A-butrol), 1,11-bis(2-methoxyethylamino)-1,11-dioxo-3,6,9-triaza-3,6,9-tris(carboxymethyl)-undecane (DTPA-BEMA), and (4-carboxymethyl)-1-phenyl-2-oxa-5,8,11-triazatridecan-13-oic acid (BOPTA) are effective magnetic resonance imaging (MRI) contrast agents when bound to a trivalent gadolinium ion.[4–7] These gadolinium(III) complexes display good relaxivity and high stability. To avoid complex dissociation, Gd(III) chelates characterized by high thermodynamic stability and kinetic inertness are commonly sought.[8–16] The acute toxicity of gadolinium(III) complexes with the linear poly(aminocarboxylate) ligands correlates well with the selectivity constant of ligand for Gd(III) over endogenously available metal ions.[15,16] The relaxation effect of a gadolinium(III) complex, the relaxivity, can be divided into two parts: (1) outer-sphere relaxivity, resulting from long-range interactions between gadolinium(III) and bulk water; (2) inner-sphere relaxivity due to short-range interactions between gadolinium(III) and inner-sphere water molecules. The inner-sphere contribution to total relaxivity depends on the number of water molecules in the inner-sphere, the proton-exchange rate, the rotational correlation time, and the electronic relaxation rate. The proton-exchange rate, as confirmed recently for several gadolinium(III) complexes, can be taken as identical to the exchange rate of all the water molecules at physiological pH.[17–19]

^{17}O NMR spectroscopy is an efficient technique for studying water-exchange rate because the oxygen of the coordinated

† Electronic supplementary information (ESI) available: tables of pM values and relaxivities; potentiometric titration curves for TTDA-PY, TTDA-HP, TTDA-H1P and TTDA-H2P; species distribution curves, plots of temperature dependence of transverse electronic relaxation rates and plots of pH dependence of conditional stability constants for Gd complexes of all four ligands and TTDA; ^1H NMR and COSY spectra of $[La(TTDA\text{-}HP)]^-$. See http://www.rsc.org/suppdata/dt/b1/b107456n/

water molecule, directly bound to the paramagnetic Gd^{3+} ion, is a more sensitive antenna than protons. Another advantage of this method is that the outer-sphere contribution to the relaxation is negligible.[20] However, the interpretation of ^{17}O NMR transverse relaxation rates has faced some problems, mainly due to the fact that the electronic relaxation parameters, obtained only from ^{17}O NMR transverse relaxation rates, are rather ill-defined. Therefore, it is desirable to determine these parameters by EPR spectroscopy as an independent technique providing direct access to transverse electronic rates.[21]

The characterization of the gadolinium(III) complex with bis(amide) derivatives of DTPA, *N′*-pyridylmethyl and *N′*-2-hydroxypropyl derivatives of DTPA and 3,6,10-tri(carboxymethyl)-3,6,10-triazadodecanedioic acid (TTDA) have been investigated in our earlier studies.[22–28] In the continuing search for gadolinium(III) chelates for use in MRI, we have modified the central carboxylate group of TTDA with 2-pyridylmethyl, 2-hydroxypropyl, 2-hydroxy-1-phenylethyl and 2-hydroxy-2-phenylethyl moieties and explored the protonation constants of these ligands, the stability constants of the metal complexes and the relaxometric investigations of gadolinium(III) chelates. This report describes the synthesis of four derivatives of TTDA, 3,10-di(carboxymethyl)-6-pyridylmethyl-3,6,10-triazadodecanedioic acid (TTDA-PY), 3,10-di(carboxymethyl)-6-(2-hydroxypropyl)-3,6,10-triazadodecanedioic acid (TTDA-HP), 3,10-di(carboxymethyl)-6-(2-hydroxy-1-phenylethyl)-3,6,10,-triazadodecanedioic acid (TTDA-H1P) and 3,10-di(carboxymethyl)-6-(2-hydroxy-2-phenylethyl)-3,6,10-triazadodecanedioic acid (TTDA-H2P) (Scheme 1), their protonation, thermodynamic, and conditional stability constants of complexes with lanthanide(III), Cu(II), Zn(II) and Ca(II) and their selectivity for Gd^{3+} over endogenously available metal ions are discussed. ^{17}O NMR shifts of the $[Dy(TTDA\text{-}PY)]^-$, $[Dy(TTDA\text{-}HP)]^-$, $[Dy(TTDA\text{-}H1P)]^-$ and $[Dy(TTDA\text{-}H2P)]^-$ complexes and water proton spin–lattice relaxivity r_1 of the $[Gd(TTDA\text{-}PY)(H_2O)]^-$, $[Gd(TTDA\text{-}HP)(H_2O)_2]^-$, $[Gd(TTDA\text{-}H1P)(H_2O)_2]^-$ and $[Gd(TTDA\text{-}H2P)(H_2O)_2]^-$ are described. Their kinetic parameters are also obtained by analysis of the ^{17}O NMR transverse relaxation rate data using the results of a single-magnetic field EPR study.

Experimental

Materials

Gadolinium oxide (>99.9%) was obtained from Aldrich Chemical Co. and oven dried at 110 °C for at least 24 h before use. All other reagents used for the synthesis of the ligands were purchased from commercial sources unless otherwise noted. Proton and ^{13}C NMR spectra and elemental analyses were used to confirm the composition of the products. ^{17}O-enriched water (10.5%) was purchased from Isotec Inc.

Preparations

Synthesis of *N,N*-bis(phthalimide)triazaoctane (DPTO). To a 500 cm^3 two-necked round-bottom flask was added phthalic anhydride (36.95 g, 249.42 mmol) and chloroform (200 cm^3). The solution was cooled to 5 °C in an ice bath and *N*-(2-aminoethyl)-1,3-propanediamine (13.92 g, 118.77 mmol) was added. The reaction mixture became slurry within 20 min and the mixture was stirred for 5 h. The pale yellow slurry was filtered with a Büchner funnel, washed with CH_3OH (4 × 60 cm^3) and then vacuum dried to give 25.43 g (51.8%) of a white solid, mp: 158.0–159.0 °C. Anal. calc. (found) for $C_{21}H_{19}N_3O_4\cdot 2H_2O$ (FW = 413.43): C, 61.01 (60.98); H, 5.61 (5.52); N, 10.16 (9.96)%. ^1H NMR ($CDCl_3$): δ 7.00 (m, 8H, ArH), 2.95 (t, 2H, ethylene backbone), 2.86, (t, 2H, propylene backbone), 2.29 (t, 2H, ethylene backbone), 2.17 (t, 2H, propylene backbone), 1.27 (p, 2H, $-NCH_2CH_2CH_2N-$).

General procedure for the reaction of DPTO with 2-picolyl chloride or (*S*)-(−)-propylene oxide. DPTO (5.0 g, 12.09 mmol) was suspended in 50 cm^3 of water, with stirring and the pH was adjusted to between 11.5 and 12.0 by addition of NaOH (2.0 mol dm^{-3}). The reaction mixture was kept at room temperature and 2-picolyl chloride (1.1 equiv) or (*S*)-(−)-propylene oxide (15% excess) was added. Then the mixture was stirred for one day after which time 6 mol dm^{-3} HCl (100 cm^3) was added to remove the protecting group. In the case of **4a** and **4b**, the crude product was purified with an AG 50W × 8 cation exchange resin column (200–400 mesh, H^+ form, 100 cm^3 of resin, 4.2 cm column diameter). All fractions containing the product were evaporated by rotary evaporation and coevaporated three times with 150 cm^3 of water to remove the excess HCl.

***N′*-(2-Hydroxypropyl)triazaoctane (TO-HP, 4a).** Yield 1.12 g, 32.6%. ^1H NMR (D_2O): δ 4.19 (m, 1H, –C*H*OH), 3.60 (m, 2H, ethylene backbone), 3.45 (m, 2H, propylene backbone), 3.32 (m, 2H, ethylene backbone), 3.31, 3.19 (t, t, 2H, propylene backbone), 3.05 (t, 2H, $-NCH_2CH(OH)-$), 2.11 (p, 2H, $-NCH_2CH_2CH_2N-$), 1.20 (d, 3H, $-CH(OH)CH_3$).

***N′*-(2-Pyridylmethyl)triazaoctane (TO-PY, 4b).** Yield 1.76 g, 42.2%. ^1H NMR (D_2O): δ 8.59, 8.35, 7.94, 7.82 (m, 4H, pyH), 4.35 (s, 2H, NCH_2py), 3.15 (s, 4H, backbone), 2.80 (m, 4H, backbone), 1.84 (p, 2H, $-NCH_2CH_2CH_2N-$).

General procedure for the reaction of 4a and 4b with *tert*-butylbromoacetate. A suspension of **4a**, **4b**, potassium carbonate (10 g, 72.35 mmol) and *tert*-butylbromoacetate (4.1 equiv) in CH_3CN (120 cm^3) was stirred at reflux for 36 h. The potassium carbonate was removed by filtering the reaction mixture with a Büchner funnel and was washed with CH_3CN (20 cm^3). The filtrate was evaporated by rotary evaporation. To the residue was added H_2O followed by extraction with chloroform (3 × 50 cm^3). The chloroform phase was evaporated under reduced pressure and 2 mol dm^{-3} HCl (50 cm^3) was added. The solution was stirred for 6 h at ambient temperature, stripped to dryness and the acid treatment repeated three times (until ^1H NMR showed complete removal of the *tert*-butyl group). In the case of salts **5a** and **5b**, the residue was dissolved in 50 cm^3 of distilled water and the solution was loaded into an AG 50W × 8 cation exchange resin column (200–400 mesh, H^+ form, 100 cm^3 of resin, 4.2 cm column diameter). All fractions containing the product were evaporated by rotary evaporation and coevaporated three times with 150 cm^3 of water to remove the excess HCl. Then the products were dissolved in 30 cm^3 of distilled water and alkalized with ammonia water to pH 11.0 and the solution applied to an AG1 × 8 anion exchange resin column (200–400 mesh, HCO_2H form, 60 cm^3 of resin, 3.0 cm column diameter). All fractions containing the products were evaporated by rotary evaporation and coevaporated three times with 200 cm^3 of water to remove the formic acid.

***N′*-(2-Hydroxypropyl)di(carboxymethyl)triazadodecanedioic acid (TTDA-HP, 5a).** Yield 1.32 g, 77.2%. Anal. calc. (found) for $C_{15}H_{27}N_3O_9\cdot 1.5H_2O$ (FW = 434.44): C, 44.24 (44.61); H, 7.83 (8.05); N, 9.67 (9.72)%. ^1H NMR (D_2O, pD 3.67): δ 3.99 (m, 1H, –C*H*OH), 3.77 (s, 4H, $-CH_2COOH$), 3.52 (s, 4H, $-CH_2COOH$), 3.26 (t, 2H, propylene backbone), 3.10 (t, 2H, ethylene backbone), 3.05 (m, 2H, ethylene backbone), 2.92 (t, 2H, propylene backbone), 2.76 (m, 2H, $-NCH_2CH(OH)-$), 2.02 (p, 2H, $-NCH_2CH_2CH_2N-$), 1.12 (d, 3H, $-CH(OH)CH_3$).

***N′*-(2-Pyridylmethyl)di(carboxymethyl)triazadodecanedioic acid (TTDA-PY, 5b).** Yield 0.96 g, 42.7%. ^1H NMR (D_2O): δ 8.68, 8.49, 7.94, 7.82 (m, 4H, pyH), 4.18 (s, 2H, NCH_2py), 4.03 (s, 4H, $-CH_2COOH$), 3.92 (s, 4H, $-CH_2COOH$), 3.47 (t, 2H, backbone), 3.25 (t, 2H, backbone), 3.04 (t, 2H, backbone), 2.71 (t, 2H, backbone), 1.90 (m, 2H, $-NCH_2CH_2CH_2N-$).

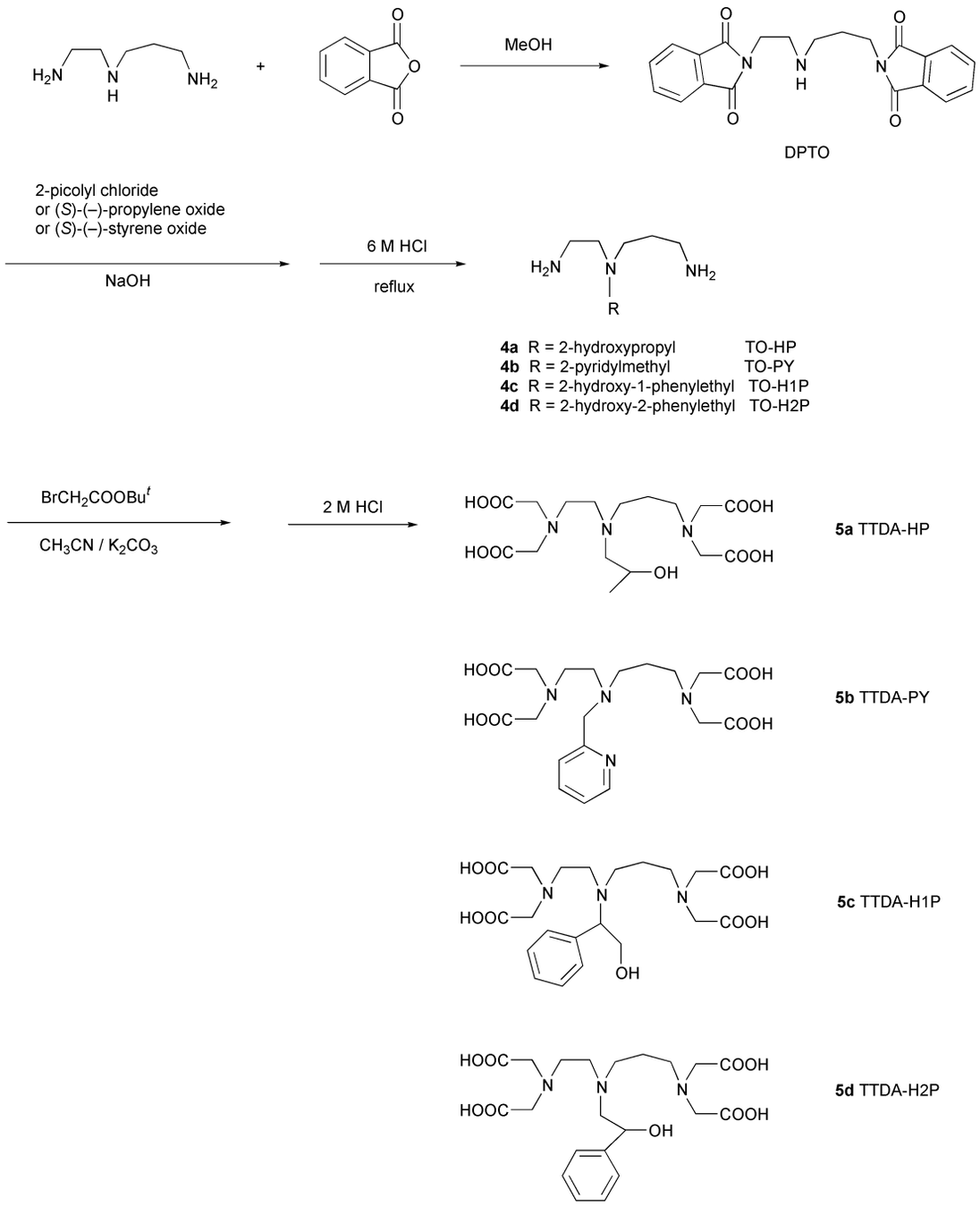

Scheme 1

Synthesis of *N*′-(2-hydroxy-1-phenylethyl)di(carboxymethyl)-triazadodecanedioic acid and *N*′-(2-hydroxy-2-phenylethyl)di-(carboxymethyl)triazadodecanedioic acid (TTDA-H1P, 5c and TTDA-H2P, 5d). Compounds **4c** and **4d** were synthesized from DPTO and (*S*)-(−)-styrene oxide (15% excess) according to the general procedure described above for **4a** and **4b**. After being vacuum dried, 1.07 g of mixed TO-H1P·3HCl and TO-H2P·3HCl was obtained as a white hygroscopic powder. Compounds **5c** and **5d** were synthesized from **4c** and **4d** according to the general procedure described above for **5a** and **5b**. After running a cation exchange resin column, the product (**5c**, **5d**) came off in 3.5 mol dm^{-3} HCl fractions. Solvent was removed from all fractions containing the product by rotary evaporation. The products were dissolved in 20 cm^3 of distilled water and alkalized with ammonia water to pH 11.0 and the solution applied to an anion exchange resin column. The product was eluted with 500 cm^3 of water, 500 cm^3 of 0.1 mol dm^{-3} formic acid, 500 cm^3 of 0.2 mol dm^{-3} formic acid, 500 cm^3 of 0.3 mol dm^{-3} formic acid, 500 cm^3 of 0.4 mol dm^{-3} formic acid and 500 cm^3 of 0.5 mol dm^{-3} formic acid. The products **5c** and **5d** came off in 0.5 mol dm^{-3} and 0.3 mol dm^{-3} formic acid, respectively. The products were evaporated separately by rotary evaporation and coevaporated three times with 200 cm^3 of water to remove the formic acid to yield 0.55 g and 0.64 g of a white hygroscopic free acid **5c** and **5d**, respectively. Anal. calc. (found) for $C_{21}H_{31}N_3O_9\cdot 1.8H_2O$ (**5c**) (FW = 501.92): C, 50.25 (50.35); H, 6.95 (7.15); N, 8.37 (8.44)%. ^{1}H NMR (D_2O, pD 4.05): δ 7.38 (m, 5H, phenyl), 4.05 (t, 1H, –C*H*CH_2OH), 3.72 (s, 2H, –CH_2COOH), 3.48 (q, 4H, –CH_2COOH), 3.23 (m, 2H, ethylene backbone), 3.18 (m, 2H, propylene backbone), 3.02, 2.88 (m, m, 2H, ethylene backbone), 2.88, 2.74, (m, m, 2H, propylene backbone), 1.96 (p, 2H, –$NCH_2CH_2CH_2N$–). Anal. calc. (found) for $C_{21}H_{31}N_3O_9\cdot 1.8H_2O$ (**5d**) (FW = 501.92): C, 50.25 (50.28); H, 6.95 (7.03); N, 8.37 (8.47)%. ^{1}H NMR (D_2O, pD 7.26), δ 7.38 (m, 5H, phenyl), 4.83 (t, 1H, –C*H*OH), 3.60 (s, 4H, –CH_2COOH), 3.52 (s, 4H, –CH_2COOH), 3.18 (m, 2H, ethylene backbone), 3.12 (m, 2H,

propylene backbone), 2.95 (m, 2H, ethylene backbone), 2.89 (m, 2H, –NCH_2CH(OH)–), 2.73 (t, 2H, propylene backbone), 1.85 (p, 2H, –NCH$_2$CH_2CH$_2$N–).

^{17}O NMR measurements

The hydration number of [Dy(TTDA-PY)]$^-$, [Dy(TTDA-HP)]$^-$, [Dy(TTDA-H1P)]$^-$ and [Dy(TTDA-H2P)]$^-$ was determined by the method of Alpoim *et al.*[29] The ^{17}O NMR spectra were recorded on a Varian Gemini 300 spectrometer at 25 °C. The induced ^{17}O shift (d.i.s.) measurements were determined using D_2O as an external standard. An equimolar solution of Dy(III) and ligand was prepared, and a stoichiometric amount of standardized NaOH was added so that the complex was fully formed. Six solutions of varying dysprosium(III) concentrations were prepared by serial dilution of the stock solution.

The measurement of the ^{17}O transverse relaxation rates was carried out with a Varian Gemini-300 (7.05 T, 40.65 MHz) spectrometer, equipped with a 5 mm probe, by using an external D_2O lock. The Varian temperature unit was used to stabilize the temperature. The value of the transverse relaxation rate was resolved by evaluating the linewidth at half-height ($\Delta\nu_{1/2}$) of the water ^{17}O signal ($R_2 = \pi\Delta\nu_{1/2}$). Solutions containing 2.6% of the ^{17}O isotope were used.

Solution preparations

Stock solutions of Ca(II), Zn(II), Cu(II) and lanthanide(III) were prepared between 0.015 and 0.025 mol dm^{-3} from nitrate salts with demineralized water (obtained by a Millipore/Milli-Q system) and standardized by titration with Na_2EDTA (disodium salt of ethylenedinitrilotetraacetic acid) or atomic absorption spectrophotometry. A stock solution was prepared by dissolving reagent grade Na_2EDTA 4.65 g and diluting it to 250 cm^3 with demineralized water. This was used as a titrant to standardize the solution of lanthanide(III) and Ca(II).[30]

Potentiometric measurements

The protonation constants of the ligands were determined by potentiometric titrations of 1.0 mmol dm^{-3} ligand solutions using an automatic titrator system. The stability constants of their complexes with Ca(II), Zn(II) and Cu(II) were also determined by direct pH potentiometry. The autotitrating system consists of a 702 SM Titroprocessor, a 728 stirrer, and a PT-100 combination pH electrode (Metrohm). The pH electrode was calibrated using three standard buffer solutions. In order to avoid any contact with CO_2, all calibrations and titrations in a glass-jacketed vessel (20 cm^3) thermostatted at 25.0 ± 0.1 °C, with an ionic strength of 0.10 mol dm^{-3} Me_4NNO_3 were carried out under a nitrogen atmosphere. A CO_2-free, 0.100 mol dm^{-3} NaOH solution was used as the titrant to minimize the change of ionic strength during the titration. The purity of the ligand was also confirmed by potentiometric titration with standard KOH. Each titration was performed at least three times.

Since the lanthanide chelates are completely or almost completely formed at low pH, their stability constant could not be determined from the normal potentiometric titration method. Therefore, these stability constants were evaluated by a ligand–ligand competition potentiometric titration in this study.[31–33] A 1 : 1 : 1 molar ratio of lanthanide(III), ligand and a reference ligand with a known metal chelate stability was titrated. A good reference ligand for the lanthanide(III) systems was found to be EDTA.[16] EDTA forms a complex with lanthanide(III) whose stability constant is accurately known.[34] The potentiometric equilibrium studies were conducted on solutions of the ligand in the absence of metal ions and then in the presence of each metal ion which the M : L ratio was 1 : 1. The δ data were obtained after additions of 0.005 cm^3 increments of standard 0.100 mmol dm^{-3} KOH solution, and after stabilization in this direction, equilibrium was then approached from the other direction by adding standard 0.100 mol dm^{-3} acid solution. The equilibria were slow to attain and it was necessary to allow about 10 min for each point of the titration where the ligand–ligand competition took place. However, complexation was usually rapid (3–5 min per point to give a stable pH reading) in the Cu(II), Ca(II) and Zn(II) solutions. The same values of the stability constants were obtained either by using the direct or the back titration. The protonation constants of the ligands were calculated using a FORTRAN computer program PKAS[35] written for polyprotonic weak acid equilibria. The overall stability constants of the various metal complexes formed in aqueous solution were determined from the titration data with the FORTRAN computer program BEST.[35] A value of 13.78 was employed for the pK_w at 25 °C. The species distribution diagrams were calculated with the FORTRAN program SPE and SPEPLOT.[35]

Relaxation time measurements

The gadolinium(III) chelate solution was prepared by combining equal molar amounts of the stock $GdCl_3$ and the ligand solution. A slight excess (3%) of the ligand was used and the solution was allowed to react for at least 2 h at room temperature to ensure full complexation. The Gd(III) chelate solutions under various pH values were prepared by combining the buffer solution with an appropriately diluted Gd(III) complex solution in a 1 : 1 (v/v) ratio. The following buffer systems were used: chloroacetic acid–NaOH (pH 2–3), acetic acid–NaOH (pH 4–5), PIPES (PIPES = piperazine-*N,N′*-bis-2-ethanesulfonic acid)–NaOH (pH 6.0–8.0) and ammonia–HCl (pH 9–10). These buffer solutions were used to maintain constant ionic strength (*i.e.* 0.10 mol dm^{-3}). The buffered Gd(III) chelate solutions were all allowed to equilibrate for at least 2 h. The pH of these solutions was determined immediately before relaxation time T_1 measurements. Relaxation times T_1 of aqueous solutions of gadolinium(III) complexes of ligands were measured to determine relaxivity r_1. All measurements were made using a NMR spectrometer operating at 20 MHz and 37.0 ± 0.1 °C (NMS 120 Minispec, Bruker). Before each measurement the spectrometer was tuned and calibrated. The values of T_1 were measured from eight data points generated by an inversion–recovery pulse sequence.

EPR measurements

The EPR spectra were recorded at the X-band (0.34 T) using a Bruker ER 200D-SRC spectrometer operated in continuous-wave mode. The samples were contained in 1 mm glass tubes. The cavity temperature was stabilized using electronic temperature control of the gas flowing through the cavity and was verified by substituting a thermometer for the sample tube. Measurements were made from 273 up to 363 K. The peak-to-peak linewidth was measured from the recorded spectra using the instrument software.

Results and discussion

Protonation constants

The potentiometric titration curves for TTDA-PY, TTDA-HP, TTDA-H1P and TTDA-H2P have been deposited as ESI (Figs. 1S–4S). Table 1 summarizes the protonation constants of TTDA-PY, TTDA-HP, TTDA-H1P, TTDA-H2P, DTPA and TTDA.[16,25] The titration curves of TTDA-PY, TTDA-HP, TTDA-H1P and TTDA-H2P show an increase at pH 9.5–5.0, 8.7–4.0, 9.0–4.0 and 9.0–4.0 at $a = 3$ (a = moles of base per mol ligand present), respectively. This is due to the large difference between the second (log K_2) and third (log K_3) protonation constants, *i.e.* 9.25 and 5.26; 8.64 and 4.45; 9.03 and 3.55; 8.83 and 4.55, respectively. The protonation constant of TTDA-PY is significantly higher than those of TTDA-HP, TTDA-H1P, TTDA-H2P and DTPA and similar to that of TTDA.

Table 1 Protonation constants of the ligands TTDA-PY, TTDA-HP, TTDA-H1P, TTDA-H2P, DTPA and TTDA at 25.0 ± 0.1 °C in aqueous Me_4NNO_3 (μ = 0.10 mol dm^{-3})

Species		log β					
H	L	TTDA-PY	TTDA-HP	TTDA-H1P	TTDA-H2P	DTPA[a]	TTDA[b]
1	1	10.37(0.06)	11.08(0.05)	10.40(0.05)	10.63(0.01)	10.49	10.60
2	1	19.62(0.02)	19.72(0.04)	19.43(0.07)	19.46(0.01)	19.09	19.52
3	1	24.88(0.04)	24.17(0.07)	22.98(0.08)	23.51(0.04)	23.37	24.64
4	1	27.90(0.01)	26.93(0.01)	25.80(0.08)	26.28(0.02)	26.01	27.44

[a] Data were obtained from refs. 16, 34 and 36. [b] Ref. 25.

Table 2 Stability constants, selectivity constants and modified selectivity constants for Gd(III), Zn(II), Ca(II) and Cu(II) complexes of TTDA-PY, TTDA-HP, TTDA-H1P, TTDA-H2P, DTPA and TTDA at 25.0 ± 0.1 °C in aqueous Me_4NNO_3 (μ = 0.10 mol dm^{-3})

Parameter	TTDA-PY	TTDA-HP	TTDA-H1P	TTDA-H2P	DTPA[a]	TTDA[b]
[GdL]/[Gd][L]	23.48(0.07)	17.33(0.05)	17.16(0.07)	17.44(0.05)	22.46	22.77
log $K_{GdL'}$ (pH 7.4)	18.65	12.39	12.52	12.76	18.14	18.04
log ([CaL]/[Ca][L])	12.02(0.03)	12.02(0.05)	12.86(0.05)	12.74(0.04)	10.75	14.45
log β_{CaHL}	7.96(0.04)	6.29(0.03)	5.30(0.03)	4.45	6.11	
log $K_{CaL'}$ (pH 7.4)	2.16	7.08	8.22	8.06	6.43	9.72
log [CuL]/[Cu][L]	20.41(0.03)	17.97(0.02)	18.40(0.09)	18.16(0.03)	21.38	19.31
log β_{CuHL}	6.18(0.02)	3.60(0.02)	3.74(0.03)	3.36	4.81	
log $K_{CuL'}$ (pH 7.4)	15.58	13.03	13.76	13.48	17.0	14.58
log [ZnL]/[Zn][L]	17.14(0.03)	15.03(0.04)	17.77(0.07)	17.37(0.03)	18.70	18.59
log β_{ZnHL}	5.86(0.02)	3.93(0.03)	5.36(0.07)	4.04	5.60	
log $K_{ZnL'}$ (pH 7.4)	12.31	10.09	13.13	12.70	14.38	13.86
selectivity [log K(Gd/Zn)]	6.34	2.30	−0.61	0.07	3.76	4.18
selectivity [log K(Gd/Ca)]	11.46	5.31	4.30	4.70	11.71	8.32
selectivity [log K(Gd/Cu)]	3.07	−0.64	−1.24	−0.72	1.08	3.46
log $K_{sel'}$	9.06	5.34	3.66	4.32	7.06	8.44

[a] Data were obtained from refs. 16, 34 and 36. [b] Ref. 25.

Replacement of the central acetate group in TTDA by the 2-pyridylmethyl group results in a decrease in log K_1 (0.23 units), an increase in log K_2 (0.33 units) and a decrease in log K_3 (0.14 units), log K_4 (0.12 units) and the ΣpK_a value (0.46 units) and by the 2-hydroxypropyl group results in an increase in log K_1 (0.48 units), a decrease in log K_2 (0.28 units), log K_3 (0.67 units) and the ΣpK_a value (1.51 units).

Thermodynamic stability constants

The potentiometric titration curves for the complexes of Ca^{2+}, Cu^{2+} and Zn^{2+} with TTDA-PY, TTDA-HP, TTDA-H1P and TTDA-H2P have been deposited as ESI (Figs. 1S–4S). The thermodynamic stability constants for metal chelate with TTDA-PY, TTDA-HP, TTDA-H1P and TTDA-H2P are presented in Table 2.[16,25,34,36] The stability constant of the Gd(III) complex with TTDA-PY is slightly higher than those of the corresponding TTDA and DTPA complexes, which may indicate a mildly higher ligand basicity for TTDA-PY. The stability constants of $[Gd(TTDA\text{-}HP)]^-$, $[Gd(TTDA\text{-}H1P)]^-$ and $[Gd(TTDA\text{-}H2P)]^-$ are very similar. The lower stability constants of the TTDA-HP, TTDA-H1P and TTDA-H2P chelates with Gd(III), Ca(II), Zn(II) and Cu(II) when compared to the DTPA, TTDA and TTDA-PY chelates may be ascribed to the weaker donor ability of the hydroxyl group oxygen atom. The stability constants of Gd(III) complexes with TTDA-HP, TTDA-H1P and TTDA-H2P are similar to that of the corresponding DEATA (*N,N*-bis(2-aminoethyl)ethylamine-*N′*,*N′*,*N″*,*N″*-tetraacetic acid)[37] (*i.e.* log K_{GdL} = 17.79). A coordination number of seven for DEATA suggests that the hydroxyl group oxygen atoms in the TTDA-HP, TTDA-H1P and TTDA-H2P ligands do not coordinate to the Gd(III) metal ion which is supported by the solution ^{1}H-NMR and COSY spectra of 0.1 mol dm^{-3} $[La(TTDA\text{-}HP)]^-$ in D_2O, pD 7.0, 25 °C, see ESI (Figs. 5S and 6S).

In the ambient-temperature (25 °C) spectrum of $[La(TTDA\text{-}HP)]^-$, the doublet at 1.31 and 1.30 ppm is assigned to the methyl protons (H_b). This doublet collapses into a singlet as the temperature increases. The protons of the terminal acetate groups (H_a) gave four AB patterns with the baricenter at 3.52 ppm (J = 40 Hz), 3.49 ppm (J = 41 Hz), 3.16 ppm (J = 42 Hz), and 2.94 ppm (J = 30 Hz), respectively. The lack of an AB pattern for proton H_c indicates that the oxygen atom of the hydroxy group is not coordinated in the lanthanide complex.

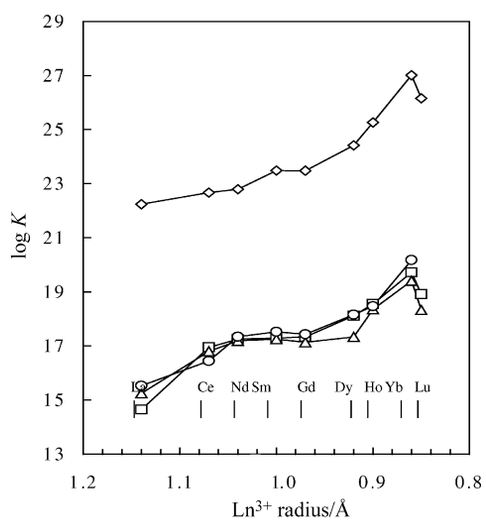

Fig. 1 Variation of stability constant with ionic radius for the lanthanide chelates of TTDA-PY (◇), TTDA-HP (□), TTDA-H1P (△) and TTDA-H2P (○).

Plots of the thermodynamic stability constants (log K_{LnL}) for lanthanide(III) chelates *versus* lanthanide(III) ionic radius are displayed in Fig. 1. The stability trend of $[Ln(TTDA\text{-}HP)]^-$, $[Ln(TTDA\text{-}H1P)]^-$ and $[Ln(TTDA\text{-}H2P)]^-$ is mainly because TTDA-HP, TTDA-H1P and TTDA-H2P are more sterically crowded or less flexible than DTPA and cannot wrap around

the smaller lanthanide(III) ions successfully. These results significantly lead to a plateau in stability for Nd(III), Sm(III), Gd(III) and Dy(III) for $[Ln(TTDA\text{-}HP)]^-$, $[Ln(TTDA\text{-}H1P)]^-$ and $[Ln(TTDA\text{-}H2P)]^-$ chelates and this is a common effect in Ln(III) solution chemistry.[38] The progressive increase in stability constants for $[Ln(TTDA\text{-}PY)]^-$ along the Ln(III) cation series is characteristic of ligand TTDA-PY because it possesses mildly higher basicity and reveals increasing stability when enhancing the charge density of the Ln(III) cation.

Conditional stability constants and selectivity constants

In Table 2 the conditional stability constants[13,16] at pH 7.4 are presented for the six ligands TTDA-PY, TTDA-HP, TTDA-H1P, TTDA-H2P, TTDA and DTPA. Their order is $[Gd(TTDA\text{-}PY)]^- > [Gd(TTDA)]^{2-} \approx [Gd(DTPA)]^{2-} > [Gd(TTDA\text{-}HP)]^- \approx [Gd(TTDA\text{-}H1P]^- \approx [Gd(TTDA\text{-}H2P)]^-$. A plot of the pH dependence of the conditional stability constants for the complexes $[Gd(TTDA)]^{2-}$, $[Gd(TTDA\text{-}PY)]^-$, $[Gd(TTDA\text{-}HP)]^-$, $[Gd(TTDA\text{-}H1P)]^-$ and $[Gd(TTDA\text{-}H2P)]^-$ has been deposited as ESI (Fig. 7S). The results of the pH dependence study of the conditional stability constants for $[Gd(TTDA)]^{2-}$ and $[Gd(TTDA\text{-}PY)]^-$ are very similar. The conditional stability constants at pH > 11 for $[Gd(TTDA)]^{2-}$ and $[Gd(TTDA\text{-}PY)]^-$ differ by a factor of $10^{0.71}$ which is similar to that at pH 7.4 ($10^{0.10}$). This demonstrates that the stability constant of $[Gd(TTDA)]^{2-}$ comes close to that of $[Gd(TTDA\text{-}PY)]^-$ at pH 7.4. The results for $[Gd(TTDA\text{-}HP)]^-$, $[Gd(TTDA\text{-}H1P)]^-$ and $[Gd(TTDA\text{-}H2P)]^-$ at pH 7.4 are very similar. These results also show that the stability constant of $[Gd(TTDA\text{-}PY)]^-$ is significantly higher than those of $[Gd(TTDA\text{-}HP)]^-$, $[Gd(TTDA\text{-}H1P)]^-$ and $[Gd(TTDA\text{-}H2P)]^-$ at pH 7.4.

The species distribution curves of $[Gd(TTDA\text{-}PY)]^-$, $[Gd(TTDA\text{-}HP)]^-$, $[Gd(TTDA\text{-}H1P)]^-$ and $[Gd(TTDA\text{-}H2P)]^-$ have been deposited as ESI (Figs. 8S–11S). The species distribution curves of $[Gd(TTDA\text{-}PY)]^-$ indicate that there is still some free Gd^{3+} at pH 1 but after pH 3 the complex is fully formed. However, the dominant species, $[Gd(TTDA\text{-}HP)]^-$, $[Gd(TTDA\text{-}H1P)]^-$ and $[Gd(TTDA\text{-}H2P)]^-$ chelates are formed at pH values larger than 5.5, 6.0 and 6.0, respectively.

The pM values[39] of ligands have been deposited as ESI (Table 1S). The pGd value of TTDA-PY resembles those of TTDA and DTPA and is larger than those of TTDA-HP, TTDA-H1P and TTDA-H2P and significantly larger than those of the corresponding $[Gd(TTDA\text{-}HP)]^-$, $[Gd(TTDA\text{-}H1P)]^-$ and $[Gd(TTDA\text{-}H2P)]^-$ chelates. The pGd value for $[Gd(TTDA\text{-}PY)]^-$ is similar to that of $[Gd(TTDA)]^{2-}$ because the protonation constants of TTDA-PY and TTDA and the stability of $[Gd(TTDA\text{-}PY)]^-$ and $[Gd(TTDA)]^{2-}$ are similar. The pM value of $[Gd(TTDA\text{-}PY)]^-$ is larger than those of $[Ca(TTDA\text{-}PY)]^{2-}$, $[Cu(TTDA\text{-}PY)]^{2-}$ and $[Zn(TTDA\text{-}PY)]^{2-}$, but $[Gd(TTDA\text{-}H1P)]^-$ and $[Gd(TTDA\text{-}H2P)]^-$ are less than those of $[Cu(TTDA\text{-}H1P)]^{2-}$ and $[Zn(TTDA\text{-}H1P)]^{2-}$, $[Cu(TTDA\text{-}H2P)]^{2-}$ and $[Zn(TTDA\text{-}H2P)]^{2-}$, respectively. Therefore, the competition among Gd^{3+}, Ca^{2+}, Cu^{2+} and Zn^{2+} with TTDA-PY seems to favor Gd^{3+} at pH 7.4, indicating that the $[Gd(TTDA\text{-}PY)]^-$ complex should be stable enough to avoid interference by Ca^{2+}, Cu^{2+} and Zn^{2+} at physiological pH.

The logarithmic selectivity constants[13,16] for TTDA-PY, TTDA-HP, TTDA-H1P, TTDA-H2P and TTDA are also shown in Table 2. The log K(Gd/Zn, Gd/Ca and Gd/Cu) values of TTDA-PY are higher than those of TTDA-HP, TTDA-H1P and TTDA-H2P indicating that TTDA-PY shows more favorable selectivity towards Gd^{3+} over Zn^{2+}, Cu^{2+} and Ca^{2+}. The complexes of Gd(III) with TTDA-HP, TTDA-H1P and TTDA-H2P have a much lower selectivity for Gd(III) over Zn(II), Cu(II) and Ca(II) which in turn leads to a high toxicity because of Gd(III) displacement by endogenous Zn(II), Cu(II) and Ca(II).[16] However, the selectivity constants, (log K(Gd/Zn)), (log K(Gd/Cu)) and (log K(Gd/Ca)), of Gd(III) complexes with TTDA-H1P and TTDA-H2P are similar; therefore the toxicity of these two complexes should probably be similar too. Table 2 also shows the modified selectivity constants ($K_{sel'}$)[16] values of TTDA-PY, TTDA-HP, TTDA-H1P, TTDA-H2P, DTPA and TTDA at pH 7.4. The log $K_{sel'}$ of TTDA-PY is higher than those of DTPA and TTDA and is significantly higher than those of TTDA-HP, TTDA-H1P and TTDA-H2P. Thus, TTDA-PY forms a gadolinium(III) complex that is more stable than those of $[Gd(TTDA\text{-}HP)]^-$, $[Gd(TTDA\text{-}H1P)]^-$ and $[Gd(TTDA\text{-}H2P)]^-$ toward transmetallation with Ca^{2+}, Zn^{2+} and Cu^{2+} metal ions at pH 7.4. In other words, the toxicity of $[Gd(TTDA\text{-}PY)]^-$ may be less than those of $[Gd(TTDA\text{-}HP)]^-$, $[Gd(TTDA\text{-}H1P)]^-$ and $[Gd(TTDA\text{-}H2P)]^-$.

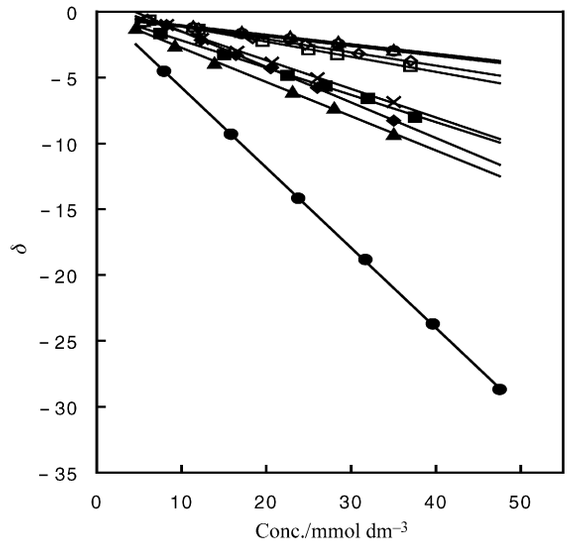

Fig. 2 The Dy(III)-induced water ^{17}O NMR shift *versus* Dy(III) chelate concentration for solutions of $[Dy(TTDA\text{-}PY)]^-$ (pH 6.3) (△), $[Dy(TTDA\text{-}PY)]^-$ (pH 4.3) (○), $[Dy(TTDA\text{-}H2P)]^-$ (pH 6.3) (◇), $[Dy(TTDA\text{-}H1P)]^-$ (pH 6.3) (□), $[Dy(TTDA\text{-}HP)]^-$ (pH 6.3) (×), $[Dy(TTDA\text{-}H2P)]^-$ (pH 4.3) (■), $[Dy(TTDA\text{-}HP)]^-$ (pH 4.3) (◆), $[Dy(TTDA\text{-}H1P)]^-$ (pH 4.3) (▲) and $DyCl_3$ (●) in D_2O at 25.0 ± 0.1 °C.

Dy(III)-Induced ^{17}O water NMR shifts

Fig. 2 shows the Dy(III)-induced water ^{17}O NMR shifts against Dy(III) chelate concentration for solutions of $DyCl_3$, $[Dy(TTDA\text{-}PY)]^-$, $[Dy(TTDA\text{-}HP)]^-$, $[Dy(TTDA\text{-}H1P)]^-$ and $[Dy(TTDA\text{-}H2P)]^-$ in D_2O at 25 °C. The slopes obtained at pH = 6.30 and pH = 4.30 are −71.2(r^2 = 0.994) and −71.1(r^2 = 0.994) for $[Dy(TTDA\text{-}PY)]^-$; −165.0(r^2 = 0.992) and −260.3(r^2 = 0.998) for $[Dy(TTDA\text{-}HP)]^-$; −148.2(r^2 = 0.997) and −269.5(r^2 = 0.992) for $[Dy(TTDA\text{-}H1P)]^-$ and −138.0(r^2 = 0.998) and −231.2 ppm dm^3 mmol^{-1}(r^2 = 0.998) for $[Dy(TTDA\text{-}H2P)]^-$, respectively. The slope for $DyCl_3$ is −608.8(r^2 = 1.000) ppm dm^3 mmol^{-1} and eight hydration numbers have been proposed for the dysprosium(III) ion.[40–42] Therefore $[Dy(TTDA\text{-}PY)]^-$, $[Dy(DTPA\text{-}HP)]^-$, $[Dy(TTDA\text{-}H1P)]^-$ and $[Dy(TTDA\text{-}H2P)]^-$ complexes at pH 6.30 and pH 4.30 contain 0.9 and 0.9; 2.2 and 3.4; 2.0 and 3.5; 1.8 and 3.0 inner-sphere water molecules per Dy(III) ion, respectively. The number of Ln(III)-bound water molecules in these complexes provides information on the coordination mode of the ligand. The coordination sites of Gd(III) ion for the $[Gd(TTDA\text{-}PY)]^-$ complex are occupied by one water molecule while eight sites are available for the TTDA-PY ligand. By binding three amine nitrogen atoms, four carboxylates and one 2-pyridylmethyl nitrogen atom of the TTDA-PY backbone, a similar coordination mode as found for the coordination sites of the previously studied bis(amide) DTPA derivative and DTPA is attained.[22,23,43,44] However, two coordination sites of Gd(III) are occupied by two water molecules and seven sites are available for TTDA-HP, TTDA-H1P

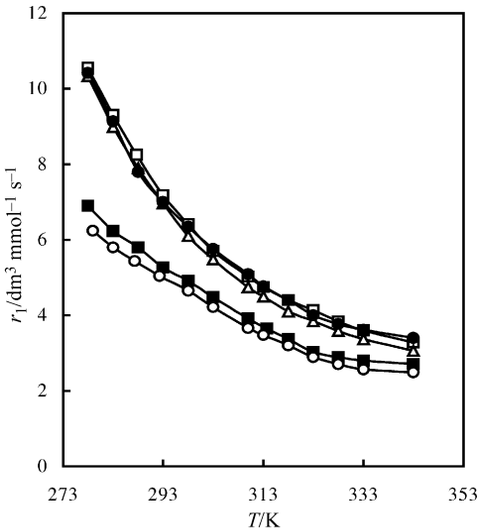

Fig. 3 Temperature dependence of the relaxivity for [Gd(TTDA-PY)]$^-$ (■), [Gd(TTDA-HP)]$^-$ (●), [Gd(TTDA-H1P)]$^-$ (□), [Gd(TTDA-H2P)]$^-$ (△) and [Gd(TTDA)]$^{2-}$ (○) at 20 MHz.

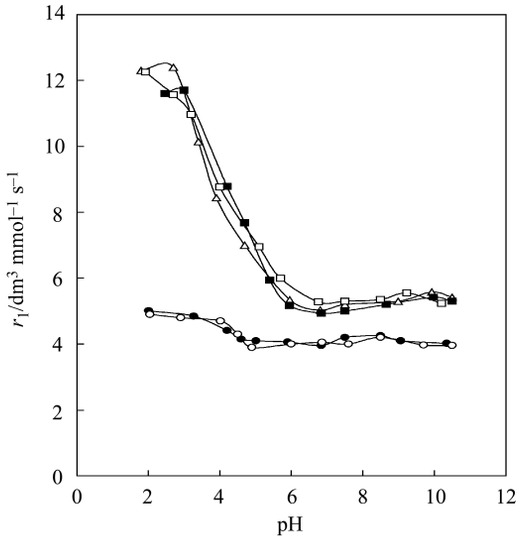

Fig. 4 pH dependence of the relaxivity for [Gd(TTDA-PY)]$^-$), (●) [Gd(TTDA-HP)]$^-$ (△), [Gd(TTDA-H1P)]$^-$ (□), [Gd(TTDA-H2P)]$^-$ (■) and [Gd(TTDA)]$^{2-}$ (○) at 20 MHz and 37 ± 0.1 °C.

and TTDA-H2P ligands. The 2-hydroxypropyl, 2-hydroxy-1-phenylethyl and 2-hydroxy-2-phenylethyl oxygen atom may not coordinate with Gd(III) metal ion in the gadolinium(III) chelates. This result is also consistent with the conclusion of the stability studies of [Gd(TTDA-HP)]$^-$, [Gd(TTDA-H1P)]$^-$ and [Gd(TTDA-H2P)]$^-$. Moreover, the previous results for the stability constant values of [Ln(TTDA-PY)]$^-$ are significantly larger than those of [Ln(TTDA-HP)]$^-$, [Ln(TTDA-H1P)]$^-$ and [Ln(TTDA-H2P)]$^-$ chelates.

Relaxometric studies of the Gd(III) complexes

The paramagnetic contribution of the solvent longitudinal relaxivity is obtained using the following equation:[45]

$$R_{1p}^{s} = Cq/[55.6(T_{1M} + \tau_M)] \quad (1)$$

Where, C is the molar concentration of the gadolinium(III) complex, q is the number of water molecules bound to metal ion, T_{1M} is the longitudinal relaxation time of the bound water protons, and τ_M is the residence lifetime of the bound water. Because of the opposite temperature dependence of T_{1M} and τ_M two cases can be considered: (1) fast water-exchange ($T_{1M} \gg \tau_M$), R_{1p}^{is} increases with decreasing temperature; (2) slow water-exchange ($T_{1M} \ll \tau_M$), R_{1p}^{is} decreases with decreasing temperature. Fig. 3 shows the temperature dependence of the relaxivity (r_1) for the [Gd(TTDA-PY)]$^-$, [Gd(TTDA-HP)]$^-$, [Gd(TTDA-H1P)]$^-$, [Gd(DTPA-H2P)]$^-$ and [Gd(TTDA)]$^{2-}$ complexes at 20 MHz in the temperature range 278–343 K. A monoexponential decrease of the observed relaxivity upon increasing the temperature in the range 278–343 K was found for these five gadolinium(III) complexes. This is characteristic of the fast chemical exchange behavior which occurs when the residence lifetime of the coordinated water molecule is much shorter than the longitudinal relaxation time of the bound water proton.

The longitudinal relaxivity r_1 values of [Gd(TTDA-PY)]$^-$, [Gd(TTDA-HP)]$^-$, [Gd(TTDA-H1P)]$^-$, [Gd(DTPA-H2P)]$^-$, [Gd(TTDA)]$^{2-}$ and [Gd(DTPA)]$^{2-}$ have been deposited as ESI (Table 2S). The r_1 value of [Gd(TTDA-PY)]$^-$ is similar to those of [Gd(DTPA)]$^{2-}$ and [Gd(TTDA)]$^{2-}$. However, the [Gd(TTDA-HP)]$^-$, [Gd(TTDA-H1P)]$^-$ and [Gd(TTDA-H2P)]$^-$ are higher than those of corresponding [Gd(DTPA)]$^{2-}$, [Gd-(TTDA)]$^{2-}$ and [Gd(TTDA-PY)]$^-$ under the same experimental conditions.[16,25] The relaxivity of a paramagnetic metal complex consists of two components: the inner-sphere and outer-sphere relaxivities. Since the basic skeleton of these ligands studied and the shapes and sizes of the gadolinium(III) complexes are similar, it is assumed that the outer-sphere relaxivities are similar. Thus, the observed relaxivity is primarily attributed to the variation in the inner-sphere contribution. The inner-sphere relaxivity is mainly dependent on the number of inner-sphere water molecules in the gadolinium(III) complex. A larger number of inner-sphere water molecules leads to a higher relaxivity r_1. The q value of the complex of gadolinium(III) with TTDA-PY is similar to those of [Gd(DTPA)]$^{2-}$ and [Gd(TTDA)]$^{2-}$ leading to almost identical r_1 values.[25,29] The relaxivity values of [Gd(TTDA-HP)]$^-$, [Gd(TTDA-H1P)]$^-$ and [Gd(TTDA-H2P)]$^-$ are higher than those of [Gd(TTDA-PY)]$^-$, [Gd(TTDA)]$^-$ and [Gd(DTPA)]$^{2-}$; this is undoubtedly due to the larger hydration number of the gadolinium(III) complex.

The relaxivity r_1 values for gadolinium(III) complexes at various pH values are shown in Fig. 4. The relaxivity r_1 curve of [Gd(TTDA-PY)]$^-$ exhibits no pH dependence over the pH range 4.0–10.5. In other words, no ligand dissociation occurred for [Gd(TTDA-PY)]$^-$ in this pH range. It is also concluded that the hydration number of [Gd(TTDA-PY)]$^-$ remains constant in this pH range. The observed relaxivity trend is in qualitative agreement with the previously obtained q values of the [Gd(TTDA-PY)]$^-$ complex at pH 4.3 and 6.3. When the pH range is less than 4 the [Gd(TTDA-PY)]$^-$ complex may undergo partial dissociation resulting in higher relaxivity. The relaxivity (r_1) trends of [Gd(TTDA-HP)]$^-$, [Gd(TTDA-H1P)]$^-$ and [Gd(TTDA-H2P)]$^-$ increase with decreasing pH values over the pH range 6.0–2.0 as shown in Fig. 4. This could be attributed to the partial dissociation of Gd(III) complexes at lower pH values. Moreover, the hydration numbers of [Gd(TTDA-HP)]$^-$, [Gd(TTDA-H1P)]$^-$ and [Gd(TTDA-H2P)]$^-$ in the pH range 4–5 are significantly higher than those at pH 6.3, see Fig. 4. Thus, the dissociation of the complexes appears to be more complete for [Gd(TTDA-HP)]$^-$, [Gd(TTDA-H1P)]$^-$ and [Gd(TTDA-H2P)]$^-$ than for [Gd(TTDA-PY)]$^-$ in the lower pH 2–6 range.

Water-exchange lifetime studies of the Gd(III) complexes

The measured peak-to-peak line widths, ΔH_{pp}, of the derivative spectrum can be related to the overall transverse electronic relaxation rate, $1/T_{2e}$, *via* eqn. (2), where g_L is the isotropic Landé g factor ($g_L = 2.0$ for Gd^{3+}).[46]

$$\frac{1}{T_{2e}} = \frac{g_L \mu_B \pi \sqrt{3}}{h} \Delta H_{pp} \quad (2)$$

The temperature dependence of transverse electronic relaxation rates at the X-band (0.34 T) at pH 7 for 50 mmol dm^{-3}

solutions of $[Gd(TTDA)]^{2-}$, $[Gd(TTDA\text{-}PY)]^{-}$, $[Gd(TTDA\text{-}HP)]^{-}$, $[Gd(TTDA\text{-}H1P)]^{-}$ and $[Gd(TTDA\text{-}H2P)]^{-}$ have been deposited as ESI (Fig. 12S). The data we obtained from each compound were fitted simultaneously with the following results of ^{17}O NMR.

Analysis of the temperature dependence of the transverse relaxation rate for the ^{17}O water nuclei is the most accurate method for evaluating the exchange lifetime of the water molecules directly coordinated to the metal in a paramagnetic Gd^{3+} chelate.[47] In principle, the exchange lifetime for the protons on the coordinated water may result either from the exchange rate of the whole water molecule ($1/\tau_M^o$) or/and from the protropic exchange rate ($1/\tau_M^H$) shown in eqn. (3).[47,48] This approach allows

$$(\tau_M)^{-1} = (\tau_M^o)^{-1} + (\tau_M^H)^{-1} \quad (3)$$

assessment of the exchange lifetime of the metal-bound water oxygen nucleus which, at neutral pH and in non-buffered solutions, corresponds to the exchange lifetime of the metal-bound water protons, *i.e.* $\tau_M = \tau_M^o$.[47,48]

The paramagnetic contribution (R_{2p}^o) to the observed transverse relaxation rate (R_{2obs}^o) of water ^{17}O nuclei at variable temperature is given by eqn. (4):

$$R_{2p}^o = R_{2obs}^o - R_{2d}^o \quad (4)$$

where the diamagnetic term R_{2d}^o is evaluated from a solution containing a diamagnetic analogue of the chelate of interest. R_{2p}^o is related to τ_M^o through the values of $\Delta\omega_M^o$ (the ^{17}O chemical shift difference between coordinated and bulk water) and R_{2M}^o (the transverse relaxation rate of the coordinated water oxygen) shown in eqn. (5):[19,49]

$$R_{2p}^o = \frac{Cq}{55.6}(\tau_M^O)^{-1}\frac{R_{2M}^{O\,2} + (\tau_M^O)^{-1}R_{2M}^O + \Delta\omega_M^{O\,2}}{\left(R_{2M}^O + (\tau_M^O)^{-1}\right)^2 + \Delta\omega_M^{O\,2}} \quad (5)$$

The temperature dependence of of $\Delta\omega_M^o$ is described by eqn. (6):[50]

$$\Delta\omega_M^O = \frac{g_L\mu_B S(S+1)B}{3k_B T}\frac{A}{\hbar} \quad (6)$$

where S is the electronic spin quantum number (7/2 for Gd^{3+}), B is the applied magnetic field strength, k_B is the Boltzmann constant, μ_B is the Bohr magneton, and $A/\hbar$ is the Gd–^{17}O scalar coupling constant, which is related to the unpaired electron spin density at the ^{17}O nucleus and is mainly dependent on the distance between the metal ion and the metal-bound ^{17}O nucleus. For gadolinium(III) with poly(aminocarboxylate) chelates this distance does not seem to vary significantly, for the gadolinium(III) complexes with TTDA, TTDA-PY, TTDA-HP, TTDA-H1P and TTDA-H2P derivatives, the same value as was reported for the closely related $[Gd(DTPA)]^{2-}$ chelate (-3.8×10^6 rad s^{-1})[19] was used.

For gadolinium(III) chelates, R_{2M}^o is dominated by the electron–nucleus scalar interaction, which is modulated by the electronic relaxation times T_{ie} (i = 1, 2) or by the exchange lifetime given by eqn. (7):[51]

$$R_{2M}^O = \frac{1}{3}\left(\frac{A}{\hbar}\right)^2 S(S+1)\left(\tau_{e1} + \frac{\tau_{e2}}{1+\omega_s^2\tau_{e2}^2}\right) \quad (7)$$

where τ_{ei} (i = 1, 2) values are the correlation times for the dynamic processes modulating the scalar interaction. Both the longitudinal and transverse electronic relaxation times (T_{1e} and T_{2e}), as well as the exchange lifetime of the metal-bound water molecule, may modulate the scalar interaction. The correlation time for this process is given by eqn. (8).

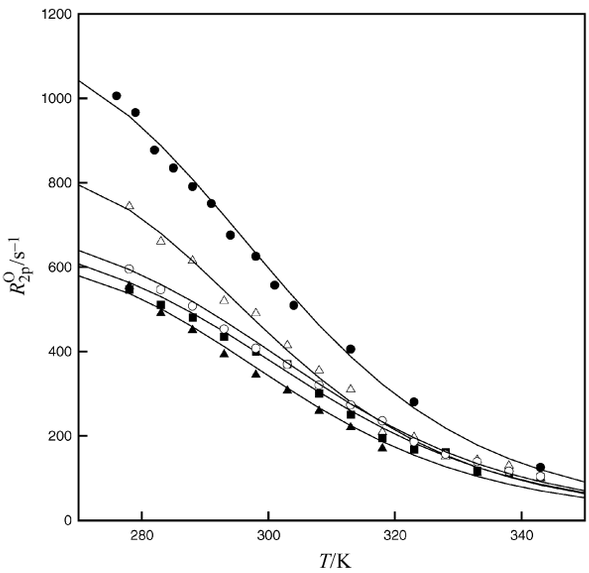

Fig. 5 Temperature dependence of the transverse water ^{17}O relaxation rate at 7.05 T and pH 7 for 50 mmol dm^{-3} solutions of $[Gd(TTDA)(H_2O)]^{2-}$ (▲), $[Gd(TTDA\text{-}PY)(H_2O)]^{-}$ (△), $[Gd(TTDA\text{-}HP)(H_2O)_2]^{-}$ (■), $[Gd(TTDA\text{-}H1P)(H_2O)_2]^{-}$ (○) and $[Gd(TTDA\text{-}H2P)(H_2O)_2]^{-}$ (●). The lines represent the simultaneous least-squares fit to all data points as described in the text.

$$\tau_{ei}^{-1} = \tau_M^{o\,-1} + T_{ie}^{-1} \quad (8)$$

For gadolinium(III) complexes, T_{ie} values are basically related to the modulation of the transient zero-field splitting (ZFS) of the electronic spin states arising from the dynamic distortions of the ligand field caused by the solvent collision and, according to McLachlan,[52] in the limit of $\omega_s\tau_v \ll 1$ they are expressed by eqns. (9) and (10):

$$T_{1e}^{-1} = \frac{1}{25}\Delta^2[4S(S+1-3)]\left[\frac{\tau_v}{1+\omega_s^2\tau_v^2} + \frac{4\tau_v}{1+4\omega_s^2\tau_v^2}\right] \quad (9)$$

$$T_{2e}^{-1} = \frac{1}{50}\Delta^2[4S(S+1-3)]\left[3\tau_v + \frac{5\tau_v}{1+\omega_s^2\tau_v^2} + \frac{2\tau_v}{1+4\omega_s^2\tau_v^2}\right] \quad (10)$$

where Δ^2 is the mean-square zero field splitting energy, τ_v is the correlation time for modulation of the zero field splitting interaction, and ω_s is the electronic Larmor frequency. This modulation may result either from rotation or from transient distortions of the complex. The temperature dependence of τ_v has an Arrhenius behavior as shown in eqn. (11):[17]

$$(\tau_j)_T^{-1} = \frac{(\tau_j^{-1})^{298.15}T}{298.15}\exp\left[\frac{\Delta H_j}{R}\left(\frac{1}{298.15} - \frac{1}{T}\right)\right] \quad (11)$$

where the subscript j refers to the two different dynamic processes involved (j = M, v) and ΔH_j is the corresponding activation enthalpy.

The transverse electronic relaxation of Gd^{3+} in solution was analyzed with the assumption that the mean transverse electronic relaxation time can be used to describe the observed line width.[21] The ZFS electronic relaxation mechanism can be due either to a permanent ZFS modulated by rotation of the complex or to a transient ZFS regulated by random distortions of the complex.

An accurate determination of the water-exchange rate is possible by measuring the ^{17}O NMR transverse relaxation rate (R_{2p}^o) as a function of temperature.[46,48] The results for

Table 3 Kinetic and NMR parameters of $[Gd(TTDA)(H_2O)]^{2-}$, $[Gd(TTDA\text{-}PY)(H_2O)]^{-}$, $[Gd(TTDA\text{-}HP)(H_2O)_2]^{-}$, $[Gd(TTDA\text{-}H1P)(H_2O)_2]^{-}$, $[Gd(TTDA\text{-}H2P)(H_2O)_2]^{-}$ and $[Gd(DTPA)(H_2O)]^{2-}$ as obtained from the simultaneous fit of ^{17}O NMR and EPR data

Complexes	$10^{19}\ \Delta^2/s^{-2}$	τ_v/ps	τ_M/ns	ΔH_v/J mol^{-1}
$[Gd(TTDA)(H_2O)]^{2-}$	4.6 ± 0.2	25 ± 1	10.6 ± 1.3	1.6 ± 1.0
$[Gd(TTDA\text{-}PY)(H_2O)]^{-}$	3.7 ± 0.2	31 ± 1	12.5 ± 1.1	1.5 ± 1.2
$[Gd(TTDA\text{-}HP)(H_2O)_2]^{-}$	9.7 ± 0.3	45 ± 2	6.7 ± 0.5	1.6 ± 0.9
$[Gd(TTDA\text{-}H1P)(H_2O)_2]^{-}$	9.2 ± 0.3	45 ± 1	7.1 ± 0.9	1.6 ± 1.0
$[Gd(TTDA\text{-}H2P)(H_2O)_2]^{-}$	5.4 ± 0.2	70 ± 2	9.1 ± 0.9	1.3 ± 1.0
$[Gd(DTPA)(H_2O)]^{2-}$ [a]	4.6 ± 0.2	25 ± 1	303 ± 35	1.6 ± 1.8

[a] Data were obtained from ref. 19.

$[Gd(TTDA)(H_2O)]^{2-}$,$[Gd(TTDA\text{-}PY)(H_2O)]^{-}$,$[Gd(TTDA\text{-}HP)(H_2O)_2]^{-}$, $[Gd(TTDA\text{-}H1P)(H_2O)_2]^{-}$ and $[Gd(TTDA\text{-}H2P)(H_2O)_2]^{-}$ complexes are plotted in Fig. 5 with the corresponding curves representing the results of the best fitting of the data according to eqns. (2)–(11). As there are a large number of parameters to be determined in the quantitative analysis of the ^{17}O NMR transverse relaxation rate (R_{2p}^{o}) *versus* T profiles, it is convenient to fix some of them. On this basis, besides the value of q and $A/\hbar$, the value of ΔH_M used for all these gadolinium(III) complexes with TTDA, TTDA-PY, TTDA-HP, TTDA-H1P and TTDA-H2P is 40 kJ mol^{-1}.[53]

For these five complexes, a good fit of the data with the parameters in Table 3 is obtained. At 298 K, the accurate estimation of τ_M^{o} values are 10.6 ns, 12.5 ns, 6.7 ns, 7.1 ns and 9.1 ns for $[Gd(TTDA)(H_2O)]^{2-}$, $[Gd(TTDA\text{-}PY)(H_2O)]^{-}$, $[Gd(TTDA\text{-}HP)(H_2O)_2]^{-}$, $[Gd(TTDA\text{-}H1P)(H_2O)_2]^{-}$ and $[Gd(TTDA\text{-}H2P)(H_2O)_2]^{-}$, respectively. These values are very close to the optimal range for the attainment of the high relaxivities expected when the molecular reorientational time of the complexes is lengthened to the nanoseconds range.[54] These five complexes are of the same order of magnitude suggesting that, in spite of their hydration number differing by one unit, the water-exchange may take place through a similar mechanism.

By varying the temperature over a wide range, R_{2p}^{o} is dominated by $1/\tau_M$ in the slow kinetic region at low temperature and is dominated by $1/\tau_{ei}$ in the fast kinetic region at high temperature. The maximum in the profiles corresponds to the translation from the slow to the fast kinetic regions. The maximum in the profile of ^{17}O NMR transverse relaxation rate (R_{2p}^{o}) *versus* T could not be found for $[Gd(TTDA)(H_2O)]^{2-}$, $[Gd(TTDA\text{-}PY)(H_2O)]^{-}$, $[Gd(TTDA\text{-}HP)(H_2O)_2]^{-}$, $[Gd(TTDA\text{-}H1P)(H_2O)_2]^{-}$ and $[Gd(TTDA\text{-}H2P)(H_2O)_2]^{-}$, which indicates that the water-exchange rate is very fast.

From Table 3, the correlation time for the modulation of the ZFS (τ_v) for $[Gd(TTDA)(H_2O)]^{2-}$, is the same as that of $[Gd(DTPA)(H_2O)]^{2-}$, but smaller than those of $[Gd(TTDA\text{-}PY)(H_2O)]^{-}$, $[Gd(TTDA\text{-}HP)(H_2O)_2]^{-}$, $[Gd(TTDA\text{-}H1P)(H_2O)_2]^{-}$, and $[Gd(TTDA\text{-}H2P)(H_2O)_2]^{-}$ complexes, indicating that the modulation of the transient zero field splitting distortions is faster for $[Gd(TTDA)(H_2O)]^{2-}$, and $[Gd(DTPA)(H_2O)]^{2-}$. Meanwhile, the electronic relaxation time values are found to be very short for $[Gd(TTDA\text{-}HP)(H_2O)_2]^{-}$ and $[Gd(TTDA\text{-}H1P)(H_2O)_2]^{-}$ mainly shown by the high value of mean-square zero field splitting energy, Δ^2.[55]

The rate of water-exchange from the inner-sphere of a metal ion is affected strongly by the substitution of one or more water molecules by a coordinated ligand. For the complexes of the first-row transition elements there are a lot of experimental data showing that multidentate ligands increase significantly the rate of exchange of the remaining water molecules.[56] Contrary to these results, the water-exchange rate was found to be lower for the $[Gd(TTDA)(H_2O)]^{2-}$, $[Gd(TTDA\text{-}PY)(H_2O)]^{-}$, $[Gd(TTDA\text{-}HP)(H_2O)_2]^{-}$, $[Gd(TTDA\text{-}H1P)(H_2O)_2]^{-}$ and $[Gd(TTDA\text{-}H2P)(H_2O)_2]^{-}$ complexes (k_{ex}^{298} = 9.4 × 10^7, 8.0 × 10^7, 1.5 × 10^8, 1.4 × 10^8 and 1.1 × 10^8 s^{-1}, respectively) than that for $[Gd(H_2O)_8]^{3+}$ (k_{ex}^{298} = 1.19 × 10^9 s^{-1}).[57] The data for $[Gd(DTPA)(H_2O)]^{2-}$, Table 3, show the same trend[58] owing to the increasing σ-donating strength of the coordinated ligand leading to an increase in the water-exchange rate.[55] However, the acetate groups are weak σ-donors and the labilizing effect of the poly(aminocarboxylate) ligands is relatively low,[56,59] resulting in a decrease in the water-exchange rate.

The mechanism and the rate of the water-exchange reaction are affected by the steric constraints of the water binding site.[60,61] The exchange lifetime of $[Gd(TTDA\text{-}PY)(H_2O)]^{-}$, $[Gd(TTDA\text{-}HP)(H_2O)_2]^{-}$, $[Gd(TTDA\text{-}H1P)(H_2O)_2]^{-}$ and $[Gd(TTDA\text{-}H2P)(H_2O)_2]^{-}$ is similar to that of $[Gd(TTDA)(H_2O)]^{2-}$ as shown in Table 3. It is interesting to find that the substitution of an acetate arm with a pyridylmethyl group, a 2-hydroxypropyl group, a 2-hydroxy-1-phenylethyl group or a 2-hydroxy-2-phenylethyl group on the linear poly(aminocarboxylate) ligand causes only a slight effect on the exchange lifetime. However, the exchange lifetime of Gd(III) complexes with these five derivatives of TTDA, TTDA-PY, TTDA-HP, TTDA-H1P and TTDA-H2P is significantly lower than that of $[Gd(DTPA)(H_2O)]^{2-}$. The $[Gd(TTDA)(H_2O)]^{2-}$ and $[Gd(DTPA)(H_2O)]^{2-}$ complexes have the same five carboxylate groups, the longer backbone of the multidentate ligand in the $[Gd(TTDA)(H_2O)]^{2-}$ and thus are pulled tightly into the first coordination sphere. This results in high steric constraints on the water binding site.[58] The overall outcome is an acceleration of the water-exchange rate by one order of magnitude. Analogous considerations can be made to account for $[Gd(EGTA)(H_2O)]^{-}$ (EGTA = 3,12-bis(carboxymethyl)-6,9-dioxa-3,12-diazatetradecanedioate).[48] In this complex, two coordinating oxygen atoms are linked by an ethylenic group, which induces severe constraints on the atoms around the site occupied by the water molecule, thus favoring the exchange process.[62] The hydroxyl group oxygen atom in $[Gd(TTDA\text{-}HP)(H_2O)_2]^{-}$, $[Gd(TTDA\text{-}H1P)(H_2O)_2]^{-}$ and $[Gd(TTDA\text{-}H2P)(H_2O)_2]^{-}$ is not found to be coordinated to the metal ion, though it causes these complexes to be less crowded, and the two inner-sphere water molecules make the water-exchange rate faster than that of $[Gd(DTPA)(H_2O)]^{2-}$.[53,58,63]

Conclusion

The octadentate poly(aminocarboxylate) ligand, TTDA-PY, forms thermodynamically stable complexes with the trivalent gadolinium cation. It does not dissociate under physiological conditions (pH 7.4), and does not exchange with Ca(II), Cu(II) or Zn(II) to an appreciable extent. From analysis of the ^{17}O NMR relaxometric properties, the replacement of the ethylene backbone with a trimethylene backbone will increase the steric constraints at the water binding site and thereby increase the water-exchange rate. $[Gd(TTDA\text{-}HP)(H_2O)_2]^{-}$, $[Gd(TTDA\text{-}H1P)(H_2O)_2]^{-}$ and $[Gd(TTDA\text{-}H2P)(H_2O)_2]^{-}$ have higher relaxivity than $[Gd(TTDA\text{-}PY)(H_2O)]^{-}$ because $[Gd(TTDA\text{-}HP)(H_2O)_2]^{-}$, $[Gd(TTDA\text{-}H1P)(H_2O)_2]^{-}$ and $[Gd(TTDA\text{-}H2P)(H_2O)_2]^{-}$ have similar water-exchange rates and sizes, the increased relaxivities are due to the presence of two water molecules in the inner coordination sphere. The thermodynamic studies have shown that $[Gd(TTDA\text{-}HP)(H_2O)_2]^{-}$, $[Gd(TTDA\text{-}H1P)(H_2O)_2]^{-}$ and $[Gd(TTDA\text{-}H2P)(H_2O)_2]^{-}$ are

not stable enough to be MRI contrast agents. On the other hand, $[Gd(TTDA\text{-}PY)(H_2O)]^-$ has adequate relaxivity, a slightly higher thermodynamic stability constant than $[Gd(DTPA)(H_2O)]^{2-}$, and an optimal water-exchange rate which make this chelate a very interesting blood pool contrast agent for MRI. Moreover, these four Gd(III) chelates may be very suitable for linking to high-molecular weight carriers.

Acknowledgements

We are grateful to the National Science Council of the Republic of China for financial support under Contract No. NSC 88-2113-M037-016.

References

1 P. Caravan, J. J. Ellison, T. J. McMurry and R. B. Lauffer, *Chem. Rev.*, 1999, **99**, 2293.
2 M. Botta, *Eur. J. Inorg. Chem.*, 2000, 399.
3 S. Aime, A. Barge, J. I. Bruce, M. Botta, J. A. K. Howard, J. M. Moloney, D. Parker, A. S. de Sousa and M. Woods, *J. Am. Chem. Soc.*, 1999, **121**, 5762.
4 E. Tóth, L. Burai, E. Brücher and A. E. Merbach, *J. Chem. Soc., Dalton Trans.*, 1997, 1587.
5 J. Platzek, P. Blaszkiewicz, H. Gries, P. Luger, G. Michl, A. Müller-Fahrnow, B. Radüchel and D. Sülzle, *Inorg. Chem.*, 1997, **36**, 6086.
6 C. F. G. C. Geraldes, A. M. Urbano, M. C. Alpoim, A. D. Sherry, K.-T. Kuan, R. Rajagopalan, F. Maton and R. N. Muller, *Magn. Reson. Imaging*, 1995, **13**, 401.
7 F. Uggeri, S. Aime, P. L. Anelli, M. Botta, M. Brocchetta, C. Haen, G. Ermondi, M. Grandi and P. Paoli, *Inorg. Chem.*, 1995, **34**, 633.
8 C. A. Chang, *Invest. Radiol.*, 1993, **28**, S21.
9 K. Kumar and M. F. Tweedle, *Pure Appl. Chem.*, 1992, **65**, 515.
10 K. Kumar, C. A. Chang and M. F. Tweedle, *Inorg. Chem.*, 1993, **32**, 587.
11 K. Kumar and M. F. Tweedle, *Inorg. Chem.*, 1993, **32**, 4183.
12 K. Kumar, C. A. Chang, L. C. Francesconi, D. D. Dischino, M. F. Malley, J. Z. Gougoutas and M. F. Tweedle, *Inorg. Chem.*, 1994, **33**, 3567.
13 K. Kumar, M. F. Tweedle, M. F. Malley and J. Z. Gougoutas, *Inorg. Chem.*, 1995, **34**, 6472.
14 C. Paul-Roth and K. N. Raymond, *Inorg. Chem.*, 1995, **34**, 1408.
15 M. F. Tweedle, J. J. Hagan, K. Kumar, S. Mantha and C. A. Chang, *Magn. Reson. Imaging*, 1991, **9**, 409.
16 W. P. Cacheris, S. C. Quay and S. M. Rocklage, *Magn. Reson. Imaging*, 1990, **8**, 467.
17 G. González, D. H. Powell, V. Tiddières and A. E. Merbach, *J. Phys. Chem.*, 1994, **98**, 53.
18 S. Aime, M. Botta, M. Fasano, S. Paoletti, P. M. Anelli, P. M. Uggeri and M. Virtuani, *Inorg. Chem.*, 1994, **33**, 4707.
19 D. H. Powell, O. M. Ni Dhubhghaill, D. Pubanz, L. Helm, Y. S. Lebedev, W. Schlaepfer and A. E. Merbach, *J. Am. Chem. Soc.*, 1996, **118**, 9333.
20 K. Micskei, L. Helm, E. Brücher and A. E. Merbach, *Inorg. Chem.*, 1993, **32**, 3844.
21 D. H. Powell, A. E. Merbach, G. González, E. Brücher, K. Micskei, M. F. Ottaviani, K. Köhler, A. von Zelewsky, O. Ya. Grinberg and Y. S. Lebedev, *Helv. Chim. Acta*, 1993, **76**, 2129.
22 Y. M. Wang, T. H. Cheng, G. C. Liu and R. S. Sheu, *J. Chem. Soc., Dalton Trans.*, 1997, 883.
23 Y. M. Wang, T. H. Cheng, R. S. Sheu, I. T. Chen and M. Y. Chiang, *J. Chin. Chem. Soc.*, 1997, **44**, 123.
24 Y. M. Wang, S. T. Lin, Y. J. Wang and R. S. Sheu, *Polyhedron*, 1998, **17**, 2021.
25 Y. M. Wang, C. H. Lee, G. C. Liu and R. S. Sheu, *J. Chem. Soc., Dalton Trans.*, 1998, 4113.
26 Y. M. Wang, Y. J. Wang, R. S. Sheu, G. C. Liu, W. C. Lin and J. H. Liao, *Polyhedron*, 1999, **18**, 1147.
27 Y. M. Wang, Y. J. Wang, G. C. Liu and Y. T. Kuo, *J. Chin. Chem. Soc.*, 1999, **46**, 551.
28 T. H. Cheng, Y. M. Wang, W. T. Lee and G. C. Liu, *Polyhedron*, 2000, **19**, 2027.
29 M. C. Alpoim, A. M. Urbano, C. F. G. C. Geraldes and J. A. Peters, *J. Chem. Soc., Dalton Trans.*, 1992, 463.
30 C. A. Chang, H. G. Brittain, J. Telser and M. F. Tweedle, *Inorg. Chem.*, 1990, **29**, 4468.
31 W. R. Harris and A. E. Martell, *Inorg. Chem.*, 1976, **15**, 713.
32 Y. Li, A. E. Martell, R. D. Hancock, J. H. Reibenspies, C. J. Anderson and M. J. Welch, *Inorg. Chem.*, 1996, **35**, 404.
33 C. H. Taliaferro, R. J. Motekaitis and A. E. Martell, *Inorg. Chem.*, 1984, **23**, 1188.
34 R. M. Smith and A. E. Martell, *Critical Stability Constants*, Plenum, New York, 1975, vol. 1–4.
35 A. E. Martell and R. J. Motekaitis, *Determination and Use of Stability Constants*, 2nd edn., VCH, New York, 1992.
36 D. L. Wright, J. H. Holloway and C. N. Reilley, *Anal. Chem.*, 1965, **37**, 884.
37 P. K. Tse and J. E. Powell, *Inorg. Chem.*, 1985, **24**, 2720.
38 P. Caravan, P. Mehrhodavandi and C. Orvig, *Inorg. Chem.*, 1997, **36**, 1316.
39 W. R. Harris, K. N. Raymond and F. L. Weitl, *J. Am. Chem. Soc.*, 1981, **103**, 1316.
40 T. Kowall, F. Foglia, L. Helm and A. E. Merbach, *J. Am. Chem. Soc.*, 1995, **117**, 3790.
41 C. Cossy, L. Helm, D. H. Powell and A. E. Merbach, *New J. Chem.*, 1995, **19**, 27.
42 C. Cossy, A. C. Barnes, J. E. Enderby and A. E. Merbach, *J. Chem. Phys.*, 1989, **90**, 3254.
43 J. A. Peters, *Inorg. Chem.*, 1988, **27**, 4686.
44 S. W. A. Bligh, A. H. M. S. Chowdhury, M. McPartlin, I. J. Scowen and R. A. Bulman, *Polyhedron*, 1995, **14**, 567.
45 T. J. Swift and R. E. Connick, *J. Chem. Phys.*, 1962, **37**, 307.
46 J. Reuben, *J. Phys. Chem.*, 1971, **75**, 3164.
47 S. Aime, M. Botta, S. G. Crich, G. Giovenzana, R. Pagliarin, M. Sisti and B. Terreno, *Magn. Reson. Chem.*, 1998, **36**, S200.
48 S. Aime, M. Botta, M. Fasano and E. Terreno, *Acc. Chem. Res.*, 1999, **32**, 941.
49 S. Aime, M. Chiaussa, G. Digilio, E. Gianolio and E. Terreno, *J. Biol. Inorg. Chem. (JBIC)*, 1999, **4**, 766.
50 N. Bloembergen, *J. Chem. Phys.*, 1957, **27**, 595.
51 L. Banci, I. Bertini and C. Luchinat, *Nuclear and Electron Relaxation*, VCH, Weinheim, 1991.
52 A. D. McLachlan, *Proc. R. Soc. London, Ser. A*, 1964, **280**, 271.
53 S. Aime, E. Gianolio, E. Terreno, G. B. Giovenzana, R. Pagliarin, M. Sisti, G. Palmisano, M. Botta, M. P. Lowe and D. Parker, *J. Biol. Inorg. Chem. (JBIC)*, 2000, **5**, 488.
54 S. Aime, M. Botta, M. Fasano and E. Terreno, *Chem. Soc. Rev.*, 1998, **27**, 19.
55 S. Deibig, E. Tóth and A. E. Merbach, *J. Am. Chem. Soc.*, 2000, **122**, 5822.
56 D. W. Margerum, G. R. Cayley, D. C. Weatherourn and G. K. Pagenkopf, in *Coordination Chemistry*, A. E. Martell, ed., American Chemical Society, Washington, DC, 1978, vol. 2.
57 R. V. Southwood-Jones, W. L. Rari, K. E. Newman and A. E. Merbach, *J. Chem. Phys.*, 1980, **73**, 5909.
58 K. Micskei, D. H. Powell, L. Helm, E. Brücher and A. E. Merbach, *Magn. Reson. Chem.*, 1993, **31**, 1011.
59 R. B. Lauffer, *Chem. Rev.*, 1987, **87**, 901.
60 D. Pubanz, G. González, D. H. Powell and A. E. Merbach, *Inorg. Chem.*, 1995, **34**, 4447.
61 N. Graeppi, D. H. Powell, G. Laurenczy, L. Zékány and A. E. Merbach, *Inorg. Chim. Acta*, 1995, **235**, 311.
62 S. Aime, A. Barge, A. Borel, M. Botta, S. Chemerisov, A. E. Merbach, U. Müller and D. Pubanz, *Inorg. Chem.*, 1997, **36**, 5104.
63 É. Tóth, L. Helm, A. E. Merbach, R. Hedinger, K. Hegetschweiler and A. Jánossy, *Inorg. Chem.*, 1998, **37**, 4104.